Available online at www.sciencedirect.com
ScienceDirect
Physics Letters A 361 (2007) 18–23
PHYSICS LETTERS A
www.elsevier.com/locate/pla

Disorder-driven phase transition in a spring-block type magnetization model

K. Kovács, Z. Néda *

Department of Physics, Babeş-Bolyai University, str. Kogălniceanu 1, RO-400084 Cluj-Napoca, Romania

Received 28 March 2006; received in revised form 8 August 2006; accepted 10 August 2006

Available online 25 September 2006

Communicated by C.R. Doering

Abstract

The critical behavior of a one-dimensional Burridge–Knopoff type spring-block model, aimed to describe magnetization phenomena, is studied by Monte Carlo type computer simulations. Disorder is introduced through randomly distributed pinning centers and the magnetization process is modeled through a relaxation dynamics. The distribution of avalanche sizes (jumps in magnetization) is studied for different disorder values. The results indicate that the model exhibits a disorder-driven phase transition. Estimates for some critical exponents and scaling laws are given.

PACS: 75.60.Ej; 75.60.-d; 05.10.-a

Keywords: Disorder-driven phase transition; Burridge–Knopoff type models; Monte Carlo simulation; Barkhausen noise

1. Introduction

Systems with quenched disorder, and disorder-induced phase transitions [1–8] represent a fascinating research field in statistical physics.

In the vicinity of a first-order phase transition there are usually three characteristic time-scales: τ_a is the characteristic time-scale of the microscopic (atomic) response of the system; τ_{th} is the characteristic time-scale of the thermal fluctuations and τ_{dr} is the characteristic time-scale of the external driving. Whenever the $\tau_a \ll \tau_{dr} \ll \tau_{th}$ relation holds between the three characteristic time-scales, we can encounter a fluctuationless or athermal first-order phase transition. In contrast, for the conventional equilibrium phase transitions the $\tau_a \ll \tau_{th} \ll \tau_{dr}$ relation holds between the characteristic time-scales.

Well-known examples for such phase transitions are the athermal solid–solid diffusionless martensitic transitions [9] or the field-induced first-order phase transition in ferromagnetic systems. For many fluctuationless phase transitions hysteresis occurs even if the system is driven extremely slowly. This suggests that hysteresis is not of kinetic nature, but it is due to the quenched disorder present in these systems. A special type of fluctuationless phase-transition occurs when the amount of quenched disorder is varied in some systems. Changing the amount of disorder will qualitatively change their behavior, so this type of fluctuationless phase transitions are named disorder-driven phase transitions. Whenever disorder-driven phase transition occurs, the system has usually history-dependent metastable evolution (hysteresis is present) and the qualitative shape of the hysteresis loop changes abruptly at the critical amount of disorder. Studying an exchange-coupled Co/CoO-bilayer magnetic structure, recently Berger et al. [6] gave also experimental evidence for the theoretically predicted disorder-driven phase transition.

Disorder-driven phase transitions were observed in many models aimed to describe magnetization phenomena. Many recent studies proved that a convenient way of treating the microscopic interactions responsible for magnetization phenomena can be done by introducing random disorder in simple magnetic models. This was done in the well-known random-field (RFIM) [1], random-bond (RBIM) [5] and random anisotropy (RAIM) [10] Ising models. These models are all capable to account for magnetic hysteresis and Barkhausen noise, and indicate also the presence of disorder-induced criticality. For a certain well-defined value of the disorder, a conventional critical point appears in these systems. On the hysteresis cycle below

* Corresponding author.
E-mail address: zneda@phys.ubbcluj.ro (Z. Néda).

0375-9601/$ – see front matter
doi:10.1016/j.physleta.2006.08.086

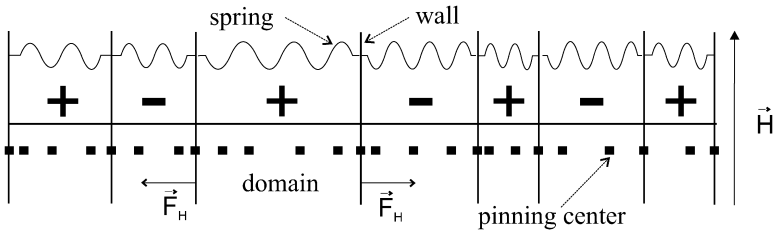

Fig. 1. Sketch of the mechanical spring-block model.

this critical amount of disorder the magnetization reversal from negative to positive saturation is abrupt. Above the critical value of the disorder the magnetization reversal takes place continuously without a giant avalanche which spans the whole system. There is thus a well-defined value of the quenched disorder in the system for which the transition between sharp and smooth magnetization reversal takes place. At this point a first-order fluctuationless phase-transition occurs. The tunable parameter is the amount of disorder and the most relevant signature of the critical state is the occurrence of power-law distributions for some characteristic quantities like avalanche-size distribution, signal energy-, duration- or area distribution on the magnetization curves.

Many other conceptually different models were also elaborated in order to capture the occurrence of criticality and power-laws in magnetization phenomena [11]. Most of them consider the motion of the domain-walls which separate magnetic domains with different orientation (see for example [12–18]).

These domain-walls can be either Bloch-walls or Néel-walls. The latter type of magnetic domain-walls are especially observed in thin and ultrathin films (see for example [19]).

Recently [20] we have introduced a model based on a simple mechanical analogy to describe magnetization related phenomena. This model captures all the necessary microscopic ingredients, and successfully reproduces the experimentally observed scaling laws for Barkhausen noise. The model is essentially a Burridge–Knopoff [21] type model, in which disorder is introduced by randomly distributed pinning centers acting on the domain-walls. In the present Letter we investigate the occurrence of the disorder-driven phase transition in this simple model.

2. The spring-block model for magnetization phenomena

The model considered by us [20] is essentially a one-dimensional (1D) spring-block system, similar to the 1D Burridge–Knopoff models [21,22] applied for the study of earthquakes. It is aimed to reproduce the accepted microscopic picture of domain-wall dynamics for 180 degree domain-walls which separate inversely oriented $(+|-|+|-|+\cdots)$ magnetic domains (Fig. 1).

The main advantage of this model is that it captures in a realistic and pedagogic manner all the main interactions that are believed to be responsible for magnetization phenomena. First, we assume that domain-walls are pinned by defects and impurities, and cannot move unless the resultant force acting on them is bigger than the strength of the F_p pinning force. Whenever the resulting force is greater than the pinning force, the wall simply jumps in the direction of the resulting force on the next pinning center. Apart of this pinning force there are two additional forces of magnetic origin acting on each domain-wall. To understand these forces let us consider the ith wall which separates the $(i-1)$th and ith domain. One of the forces acting on this domain-wall, F_H, results from the magnetic energy (called Zeeman-energy) of the domains $i-1$ and i in an external magnetic field H and it is easy to realize (see [20]) that this force has the form:

$$F_H = (-1)^i \beta \cdot H, \tag{1}$$

with β a constant. For positive (negative) values of the external magnetic field this force tends to increase domains oriented in the $+$ $(-)$ direction. The second type of magnetic force, F_m, acting on both sides of the domain-walls, is due to the magnetic self-energy of each domain. This force tends to minimize the length of each domain. It can be easily proved ([20]) that F_m is proportional with the length of the considered domain x_i

$$F_m = -f_m x_i. \tag{2}$$

The constant f_m is an important coupling parameter. This term models the demagnetization effect.

The system of the F_p, F_m and F_H forces can be now easily mapped on a one-dimensional spring-block Burridge–Knopoff type model [21].

The main elements in this mechanical analogy (Fig. 1) are randomly distributed pinning centers, rigid walls on the pinning centers (modeling domain-walls) separating $+$ and $-$ oriented domains and springs between the walls (modeling the F_m forces). We assume that the strength of the pinning centers (pinning forces), F_p, are randomly distributed following a normal distribution. These pinning centers behave as static friction forces acting on domain-walls. Whenever the resulting force on a domain-wall exceeds the pinning force, the wall will jump in the direction of the resultant force on the next pinning center (if this is empty). Different walls are not allowed to occupy the same pinning center. This constraint implies that the number of magnetic domains and domain-walls are kept constant and are thus a priori fixed within this model. Domains cannot totally disappear and new domains cannot appear during magnetization phenomena. This constraint implies also that total magnetization cannot be completely reached. Whenever the number of pinning centers is much larger than the number of domain walls (which is our case) the difference from the

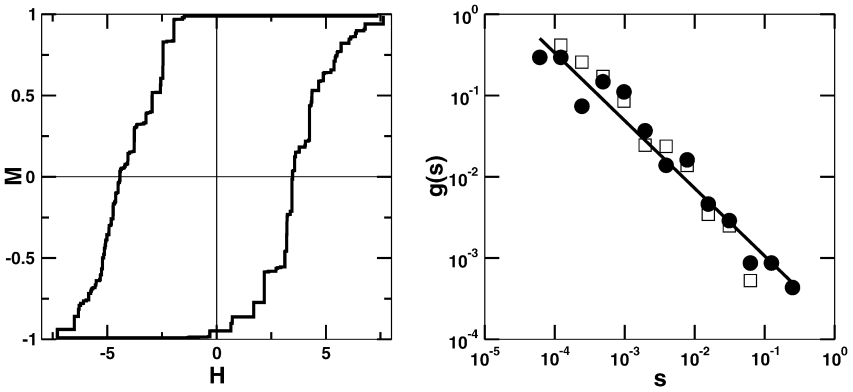

Fig. 2. Hysteresis loop (left) and corresponding jump-size distribution (right) in the vicinity of the critical regime. The power-law fit for the jump-size distribution indicates a scaling exponent −0.83. Other parameters of the simulations are: $N_p/N_w = 100$, $N_p = 7000$, $L = 7$, $\sigma = 0.4$, $f_m = 10$ and $dH = 0.001$.

achieved and total magnetization is negligible (in our case the relative difference is less than 1%).

The elastic springs connecting the walls are ideal with zero equilibrium length and tension linearly proportional with their length. The tension in the elastic springs will reproduce the F_m forces. Beside the pinning forces and the tensions in the springs there is an extra force acting on each wall. The strength of this force is proportional with the applied magnetic field's intensity. It has the same magnitude for all walls, however its direction is inverse for the $+|-$ and $-|+$ walls. This force reproduces the F_H magnetic forces. The main differences relative to the classical Burridge–Knopoff type models [21,22] is that in our case the driving force acting on the blocks has different orientations for the neighbors, and the second layer of springs which connects the sliding blocks to the driving force is absent.

Modeling magnetization phenomena with this mechanical model is straightforward. First N_p pinning centers are randomly distributed on a fixed length (L) interval, and their strengths are assigned. Than a fixed N_w number of walls are randomly spread over the pinning centers ($N_w \ll N_p$) and connected by ideal springs having the same elastic constant. Neighboring domains (separated by the walls) are assigned opposite magnetic orientation. The dynamics imposed is aimed to reproduce real magnetization phenomena. The system is driven through several complete magnetization–demagnetization cycles (hysteresis loops) by increasing and decreasing the value of H (and correspondingly F_H) using a relaxation dynamics for a given H value. Whenever for a given wall $|F_H + F_m| > F_p$ the wall will jump in the direction of the resultant force on the next pinning center. If this pinning center is occupied by another domain-wall, the wall will remain on its original place. For a given H value we consider that equilibrium is reached when no wall can move anymore. We assume that the time needed for the system to achieve equilibrium is zero. It is important to note that one event (jump) can trigger many other events leading to avalanche-like processes. The order in which the position of the walls is updated is random. The value of the F_H external force is increased step-by-step (corresponding to an increasing H magnetic field intensity), and for each new F_H value an equilibrium position of the system is searched. In each equilibrium configuration one can calculate the total magnetization of the system as:

$$M = \sum_i l_i \cdot s_i \tag{3}$$

where l_i is the length of domain i, and s_i is its orientation: $+1$ for positive orientation, and -1 for negative orientation.

The parameters of the model are: N_p—the number of pinning centers; N_w—the number of domain-walls (usually $N_w \ll N_p$); the geometrical size of the sample L; the standard deviation σ of the strength for pinning forces; f_m, the coupling constant between the neighboring domain-walls (elastic constant of the springs) and the dH driving rate of the external magnetic field (change in H for one simulation step) which is usually taken very small (quasi-static driving). The parameter β in the equation for F_H (1) is taken as unity, fixing by this the units for the relevant forces.

During the simulation we focus on the variation of the magnetization, constructing the shape of the hysteresis loop and jump-size distribution. The hysteresis loop is the history-dependent relation between the magnetization M and the external magnetic field H when the value of H is successively increased and decreased. The jump-size distribution ($g(s)$) is the distribution function of the abrupt jumps in M throughout many hysteresis loops. In our previous study [20], we have proved that for reasonable parameter values the model reproduces well the shape of hysteresis loops and the statistics of Barkhausen jumps. As an example on Fig. 2 we have plotted a characteristic hysteresis loop and the corresponding jump-size distribution in the critical regime (where the jump-size distribution follows a power-law).

In a wide range of parameters (for example parameters as in Fig. 2 and $\sigma \geqslant \sigma_{\text{crit}}$) the shape of the obtained hysteresis curves satisfies the expectations for real magnetization phenomena. The qualitative shape of the hysteresis curves are quite stable and one can detect many discrete jumps with largely different sizes. The effects of the variation of the free parameters of the model are extensively discussed in our previous work [20].

As it was shown also in [20] the model exhibits a fair statistics for Barkhausen noise. It has also the necessary requirements for the occurrence of a fluctuationless phase transition. The characteristic time-scales of the model system are: $\tau_a = 0$

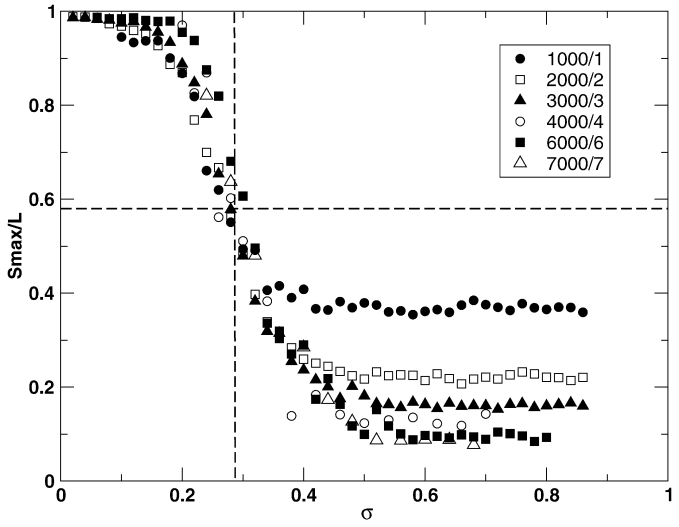

Fig. 3. Relative size of the largest avalanche as a function of the disorder for fixed pinning center density ($N_p/L = 1000$) and different system sizes: $L = 1$, $L = 2$, $L = 3$, $L = 4$, $L = 6$ and $L = 7$. Other parameters of the simulations are: $N_p/N_w = 100$, $f_m = 10$ and $dH = 0.001$.

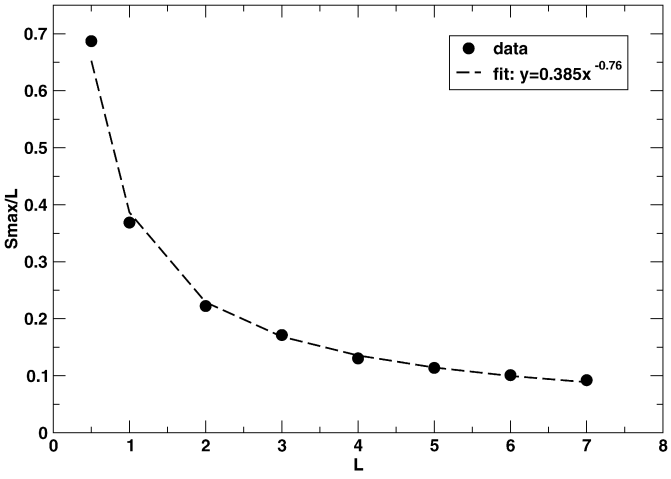

Fig. 4. Relative size of the largest avalanche at $\sigma > \sigma_{\text{crit}}$ disorders for fixed pinning center density ($N_p/L = 1000$) and different system sizes: $L = 0.5$, $L = 1$, $L = 2$, $L = 3$, $L = 4$, $L = 5$, $L = 6$ and $L = 7$. Other parameters of the simulations are: $N_p/N_w = 100$, $f_m = 10$ and $dH = 0.001$. The dashed-line indicates the best power-law fit.

(instant response), slow driving rate and zero temperature, which means that $\tau_{\text{th}} \to \infty$. Thus the relation $\tau_{\text{a}} \ll \tau_{\text{dr}} \ll \tau_{\text{th}}$ holds. Here we investigate the disorder-driven phase transition which should appear while the amount of disorder is varied in the system. This phase transition should be observable by studying the size of the largest avalanche as a function of the amount of quenched disorder introduced by the randomly distributed pinning centers. The relevant order parameter is thus the relative size of the maximal avalanche. It is computed by averaging over several hundreds of different realizations of the quenched disorder, keeping all parameters of the model fixed.

3. Simulation results for the disorder-driven phase transition

As it is known from previous studies on RFIM, RBIM and RAIM [1,5,10] the amount of disorder in the model has a crucial role on the statistical properties of the obtained jumps in magnetization. For low and very strong disorder values the jump-size distribution does not exhibit scaling property. Usually there is a critical amount of disorder for which the jump-size distribution has power-law decay.

In the present model the disorder is induced by the randomly distributed pinning centers. The amount of disorder can be controlled in two manner: either by varying the average distance, L/N_p, between the pinning centers (inverse of the density of the pinning centers N_p/L) or by changing the standard deviation σ of their strength's distribution. Here, we use both of these methods and expect qualitatively similar results. We will use the parameters given in the caption of Fig. 2, and vary σ or N_p/L.

First, by keeping the density of the pinning centers constant, the order parameter (the maximum size of the avalanches), $S_{\max}/L$, versus σ is studied. For various system sizes the simulation results are plotted in Fig. 3. The shape of the curves indicates that the expected disorder-induced phase transition occurs. The results show that for low values of the disorder ($\sigma < \sigma_{\text{crit}}$) huge avalanches arise which sweep through the whole system. This means that the magnetization reverses abruptly at a certain intensity of the driving field. There is a critical amount of disorder σ_{crit} where the curves have their inflection point. In the neighborhood of σ_{crit} the avalanche sizes will drop drastically.

Fig. 3 suggest that by increasing the system sizes the curves ($S_{\max}/L$ versus σ) show similar behavior, the location of the inflection point does not move and the two phases become more and more distinct.

For high amount of disorder ($\sigma > \sigma_{\text{crit}}$) there is no possibility for spanning avalanches to occur. The relative size of the largest avalanche in this case is much smaller. For an infinite system one would expect that the relative size of the non-spanning avalanches should approach zero. Due to the fact that computer simulations were performed with finite system sizes, this quantity is naturally greater than zero. It is quite simple to prove that for infinite system sizes and for high values of σ there is a clear tendency for the $S_{\max}/L$ quantity to approach zero. In order to do this we considered the case of ($\sigma = 0.8 \gg \sigma_{\text{crit}}$) and plotted the value of $S_{\max}/L$ as a function of system size. Results are shown in Fig. 4 and are well fitted by a power-law with exponent -0.76. The power-law nature of this curve supports our expectation that for $\sigma > \sigma_{\text{crit}}$ indeed the relative size of the order parameter $S_{\max}/L$ goes to zero as the system size tends to infinity.

Using polynomial fits we located the inflexion point of the $S_{\max}/L$ versus σ curves. This is indicated in Fig. 3 by dashed lines. Results suggest that regardless of the system size the critical amount of disorder for this particular pinning center density is the same, namely $\sigma_{\text{crit}} = 0.28 \pm 0.02$. The corresponding relative size of the percolating avalanche is: $S_{\max}/L = 0.59 \pm 0.03$. This avalanche size at criticality is in good agreement with the result reported by Vives and Planes [10].

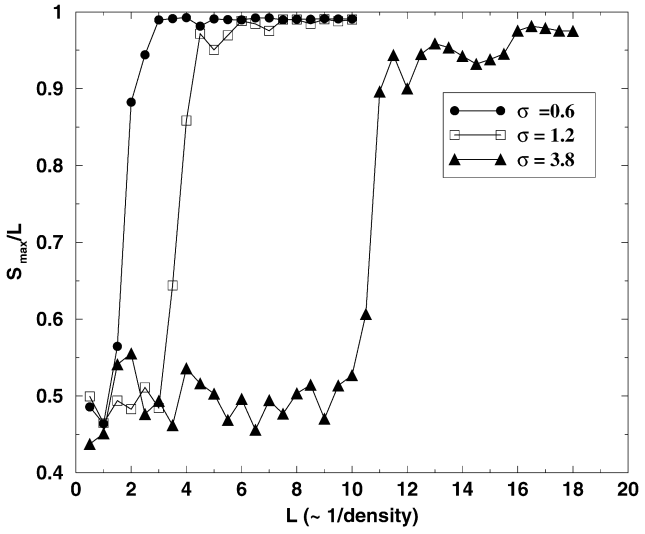

Fig. 5. Relative size of the largest avalanche as a function of the average distance between the pinning centers. The three curves correspond to three different σ values. Other parameters of the simulations are: $N_p/N_w = 100$, $N_p = 1000$, $f_m = 10$ and $dH = 0.001$.

We study now this disorder-induced phase transition as a function of the average distance (L/N_p) between the pinning centers. In the simulation the number of pinning centers were kept constant ($N_p = 1000$) and the size of the system, L, varied. The phase transition should be observable by plotting the relative size of the maximal avalanche (order parameter), $S_{\max}/L$, versus L (which is proportional with 1/density). Results for three different σ values are given on Fig. 5.

The graphs from Fig. 5 indicate that disorder-driven phase transition is present again and clearly observable for a wide range of σ values. As the strength of the disorder in the pinning force values is increased (σ is increased), the phase transition occurs for lower and lower pinning center densities, i.e. L_{crit} increases with increasing σ values. This result is not surprising at all, since the total amount of quenched disorder in the system depends linearly both as a function of σ and N_p/L. An immediate estimate for the total amount of disorder would be: $\sigma N_p/L$, which would yield the

$$L_{\text{crit}} \propto \sigma \tag{4}$$

scaling law for the L_{crit} phase transition point. The transition point L_{crit} can be estimated from the coordinates of the inflection point in the $S_{\max}/L$ versus L curves. After studying the disorder-driven phase transition for several σ values the validity of (4) can be studied. On Fig. 6 we plotted the computed L_{crit} values as a function of σ. The clearly visible linear trend proves our scaling hypothesis.

4. Discussion and conclusions

First let us emphasize a few advantages of using this spring-block model relative to the other well-known models, like the RFIM [1,2].

The RFIM considers scalar spins $s_i = \pm 1$ on a hypercube lattice. Nearest neighbors are coupled ferromagnetically (J), a

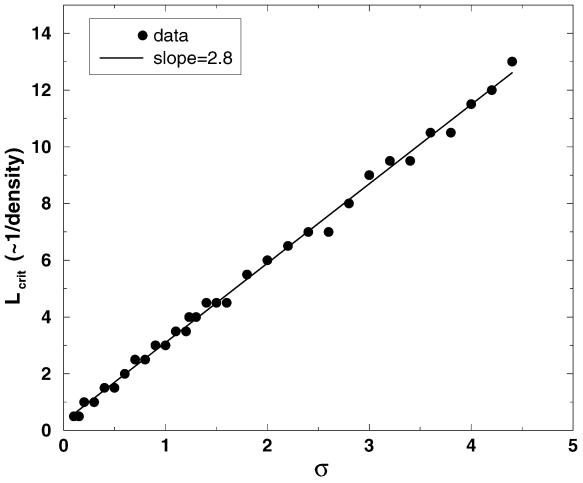

Fig. 6. Scaling of the inflection point location (obtained from the $S_{\max}/L$ versus $1/L$ curves) for different σ values. Data indicates a linear scaling with slope 2.8. Other parameters of the simulations are: $N_p/N_w = 100$, $N_p = 1000$, $f_m = 10$ and $dH = 0.001$.

random field is associated with each site (h_i), and the whole system is exposed to a magnetic field (H). The Hamiltonian is:

$$\mathcal{H} = -J \sum_{\text{n.n.}} s_i s_j - \sum_i (H + h_i) s_i. \tag{5}$$

As one can see from the Hamiltonian (5), the RFIM considers only three basic interactions: ferromagnetic coupling, interaction with the external driving field and the disorder introduced through the random fields. RFIM like many of the previous models does not account for the demagnetization effect. A second advantage of our model is the pedagogically useful mechanical analogy with the spring-block system, though it contains all the necessary microscopic ingredients needed to reproduce magnetization phenomena. Despite all of the advantages the spring-block model is far from being perfect. The main disadvantages are the fixed number of domain walls, the absence of temperature as a parameter, and the absence of real time in the dynamics (relaxation is assumed to be instantaneous in time for each magnetic field value).

A fundamental difference between RFIM (or other spin-type models) and the spring-block model is that the latter shows disorder-induced phase transition for a non-trivial disorder amount even in the simple one-dimensional case. Previous work on RFIM (see for example [2]) report the existence of such kind of phase transition in three and higher dimensions. In the RFIM in one dimension a transition-like curve is obtained in finite systems (Fig. 7). A finite-size analysis suggests however, that the critical amount of disorder tends to infinity for infinite system sizes. Moreover, the shape of the $S_{\max}(\sigma)$ curves indicates a less and less obvious transition-point (smaller slope) while the system size is increased. This behavior is different from the one observed in our spring-block model (Fig. 3), where the transition point is stable and in the vicinity of the critical amount of disorder the $S_{\max}(\sigma)$ curves gets sharper as the system size is increased.

In conclusion, in the present Letter a one-dimensional Burridge–Knopoff type magnetization model was studied from the

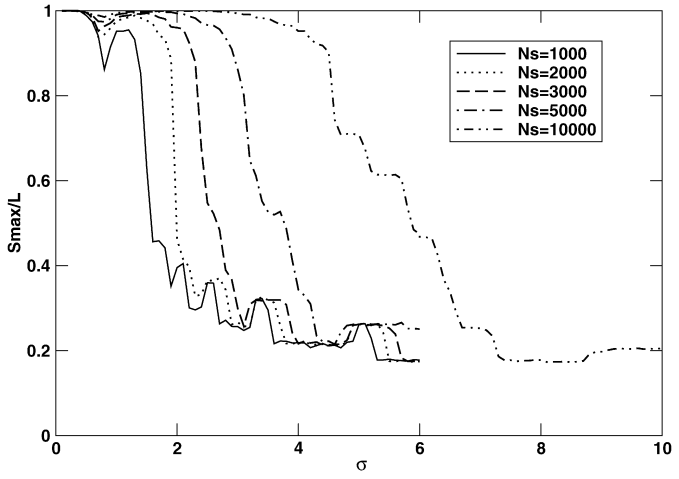

Fig. 7. Relative size of the largest avalanche as a function of the disorder in the one-dimensional RFIM for different system sizes: 1000, 2000, 3000, 5000 and 10000 spins. Coupling constant $J = 1$, driving rate $dH = 0.001$.

viewpoint of the disorder-driven phase transition. The quenched disorder was introduced by randomly distributed pinning centers, acting as static friction forces on the domain-walls. The amount of disorder could be controlled either by changing the density of the pinning centers N_p/L, or by varying the standard deviation σ of their strength. The system was driven along many hysteresis loops and the statistics of the jumps in magnetization (avalanche sizes) was computed. As relevant order parameter the relative size of the maximum avalanche (maximum jump in magnetization) $S_{\max}/L$, was considered. Disorder-induced phase transition was observed both as a function of σ and N_p/L. At criticality (critical amount of disorder) we found that the statistics of the jumps (avalanches) in magnetization follows scaling properties. For low amount of disorder (smaller than the critical amount) the system evolves with big, so-called spanning avalanches $S_{\max}/L \to 1$. For high amount of disorder (bigger than the critical amount) the system evolves with many small avalanches $S_{\max}/L \to 0$.

The disorder-induced phase transition found in our simple one-dimensional mechanical model is very similar with the one found in earlier higher-dimensional models aimed to describe magnetization phenomena and Barkhausen noise (RFIM [1], RBIM [5] and RAIM [10]). Here we have shown that the fluctuationless phase transition can be observed also in one-dimensional out-of-equilibrium systems.

Our earlier studies on this model [20] proved that at criticality the model is successful in describing the statistics of Barkhausen noise. In the present work in the framework of the disorder-induced phase transition we have given a deeper understanding for what criticality means in our model. It is also shown that criticality can be reached for several parameter values, characterized by a scaling law between σ and the density of the pinning centers.

Acknowledgements

The present work was supported by Grant CNCSIS 41/183 and Grant CNCSIS 4/31.

References

[1] J.P. Sethna, K. Dahmen, S. Kartha, J.A. Krumhansl, B.W. Roberts, J.D. Shore, Phys. Rev. Lett. 70 (1993) 3347.
[2] O. Perkovic, K. Dahmen, J.P. Sethna, Phys. Rev. B 59 (1999) 6106.
[3] O. Perkovic, K. Dahmen, J.P. Sethna, Phys. Rev. Lett. 75 (1995) 4528.
[4] A. Travesset, R.A. White, K.A. Dahmen, Phys. Rev. B 66 (2002) 024430.
[5] E. Vives, A. Planes, Phys. Rev. B 50 (1994) 3839.
[6] A. Berger, A. Inomata, J.S. Jiang, J.E. Pearson, S.D. Bader, Phys. Rev. Lett. 85 (2000) 4176.
[7] A.W. Sadvik, M. Vekic, Phys. Rev. Lett. 74 (1995) 1226.
[8] J. Marcos, E. Vives, L. Manosa, M. Acet, E. Duman, M. Morin, V. Novak, A. Planes, Phys. Rev. B 67 (2003) 224406.
[9] W. Cao, J.A. Krumhansl, R.J. Gooding, Phys. Rev. B 41 (1990) 11319.
[10] E. Vives, A. Planes, Phys. Rev. B 63 (2001) 134431.
[11] G. Durin, S. Zapperi, cond-mat/0404512.
[12] B. Alessandro, C. Beatrice, G. Bertotti, A. Montorosi, J. Appl. Phys. 68 (1990) 2908.
[13] O. Narayan, Phys. Rev. Lett. 75 (1996) 3855.
[14] S. Zapperi, P. Cizeau, G. Durin, H.E. Stanley, Phys. Rev. B 58 (1998) 6353.
[15] P. Cizeau, S. Zapperi, G. Durin, H.E. Stanley, cond-mat/9709300.
[16] G. Durin, P. Cizeau, S. Zapperi, H.E. Stanley, J. Phys. IV (France) 8 (1998) Pr2-319.
[17] G. Durin, S. Zapperi, cond-mat/9808224.
[18] J.S. Urbach, R.C. Madison, J.T. Markert, Phys. Rev. Lett. 75 (1995) 276.
[19] A. Berger, H.P. Oepen, Phys. Rev. B 45 (1992) 12596.
[20] K. Kovács, Y. Brechet, Z. Néda, Model. Simul. Mat. Sci. 13 (2005) 1341.
[21] R. Burridge, L. Knopoff, Bull. Seismol. Soc. Amer. 57 (1967) 341.
[22] J.H.E. Cartwright, E. Hernandez-Garcia, O. Piro, Phys. Rev. Lett. 79 (1997) 527.